Effective ellipsometric thickness of an interfacial layer

C. M. Marques

Cavendish Laboratory, Madingley Road, Cambridge CB3 OHE, UK, and Institut Charles Sadron, 6, Rue Boussingault, 67083 Strasbourg Cedex, France

J. M. Frigerio and J. Rivory

Laboratoire d'Optique des Solides, Université Pierre et Marie Curie, 4, Place Jussieu, 75232 Paris Cedex 05, France

Received January 15, 1991

We calculate the effective ellipsometric thickness d and index of refraction δn of interfacial inhomogeneous layers. Exact formulas are derived in the limit of zero contrast for the two usual geometries in which the light travels toward the surface from the air–liquid medium or from the substrate. d and δn are in general functions of the incident vector q, and, for small-q values and a thin layer, these effective parameters follow a parabolic dependence in q, from which the first four moments of the layer profile can be obtained. We discuss the applicability of this method for different families of profiles. We also test its predictions against the effective thickness and refractive index obtained by the numerical integration of the Maxwell equations, for the parabolic profile describing a grafted layer of polymers.

1. INTRODUCTION

Ellipsometry is nowadays a well-established technique that allows for the study of the structure of interfaces.[1] The typical experimental situation is that of a light beam traveling from a medium of constant refractive index n_0 to a different medium of constant index n_2 through an interfacial region of a spatially varying refractive index n_1.[2] This discontinuity in the optical properties of the medium creates a reflected wave whose intensity and polarization give a measure of the reflectance of the interface. The quantity measured by an ellipsometry experiment is the (complex) ratio ρ of the two reflectances R_s and R_p associated with the two polarization states **s** and **p**, respectively perpendicular and parallel to the plane of incidence:

$$\rho = R_p/R_s = \exp\{i\Delta\}\tan\psi. \tag{1}$$

The aim of our study is to investigate the possibility of reconstructing the spatial variation of the index of refraction from the experimental data ψ and Δ. This is not possible in general; one thus needs first to calculate the expected values of the ellipsometric coefficients for a given profile and then to compare them with the experimental data. The analytical expressions for the variation of ψ and Δ with the angle of incidence are available only for a small number of profiles,[1,3] but for a given arbitrary profile it is possible to integrate the Maxwell equations numerically and extract ψ and Δ. One useful representation of the interface structure is the slab model, where the index of refraction is given by

$$\begin{aligned} n &= n_0 \quad \text{if } z > d, \\ n &= n_1 \quad \text{if } 0 < z < d, \\ n &= n_2 \quad \text{if } z < 0. \end{aligned} \tag{2}$$

The bulk values n_0 and n_2 being known, one single measurement at oblique incidence allows for the determination of the effective thickness d and the effective refractive index n_1 from the ellipsometric coefficients ψ and Δ.[4] The simplicity of the method and its straightforward implementation on numerical calculators (the method is included in most of the built-in software packages for ellipsometers) contributed to the accumulation over the years of a large amount of data on effective thicknesses and indices for a variety of systems. It is thus of interest to discuss the type of information about the profile that is contained in these parameters. Clearly, when the actual profile has the form of the index step described by the slab model, the values for d and n_1 extracted from different measurements at different incidence angles coincide. In general, for a given profile, if it is not too thin, the experimental values of d and n_1 are a function of the angle at which the measurement is performed. We study here how this angle dependence is related to the index profile at the level of the Born approximation. In Section 2 we derive the central result of this paper relating the effective thickness and index of an arbitrary profile to its sine and cosine Fourier transforms for the two usual working geometries described above (light traveling toward the surface from the air–liquid medium or from the substrate). In Section 3 we extract the small wave-vector expansions from these relations and enlighten the specificity of this method by applying it to different families of profiles. In Section 4 we compare the predictions of the Born approximation against the numerical results obtained for a parabolic profile describing a polymer grafted layer.

2. EFFECTIVE THICKNESS AND INDEX OF AN ARBITRARY PROFILE

Two typical experimental geometries of an ellipsometry measurement are sketched in Fig. 1. The first situation [Fig. 1(a)] corresponds to a light plane wave traveling from a medium of constant refractive index n_0 to a medium of a

0740-3224/91/122523-06$05.00

larger constant index n_2 through the interfacial region of spatially varying refractive index. The second situation [Fig. 1(b)] corresponds to the reverse case, in which the light travels from the glass (n_2) to the air–liquid bath (n_0). Here there is a maximum angle above which total reflection occurs, i.e., an angle at which the component of the wave vector normal to the interface [$q = n_0(2\pi/\lambda)\cos\phi_0$] vanishes if $n_2 > n_0$. In this geometry it is thus possible to explore accurately the region of angles (close to total reflection) where that component is small. In a previous paper Charmet and de Gennes[2] calculated the reflectance of a diffuse layer for the first experimental geometry within a Born (linear) approximation. We now recall their results and calculate the ellipsometric coefficients for an experiment performed in the second configuration.

A. Ellipsometric Coefficients in the Born Approximation

We consider first the profile

$$\begin{aligned} n &= n_0 \qquad z \to \infty, \\ n &= n_1(z) \qquad z > 0, \\ n &= n_2 \qquad z < 0 \end{aligned} \tag{3}$$

and the equations ruling the propagation of the electric and magnetic fields E and H, which are the natural variables associated with the s and p waves:

$$\begin{aligned} &\frac{d^2E}{dz^2} + \left[\left(\frac{2\pi}{\lambda}\right)^2 n^2 - q_x^2\right]E = 0 \qquad \text{polarization } s, \\ &\frac{d^2h}{dz^2} + \left[\left(\frac{2\pi}{\lambda}\right)^2 n^2 - q_x^2 - n\frac{d^2}{dz^2}n^{-1}\right]h = 0 \qquad \text{polarization } p, \end{aligned} \tag{4}$$

where q_x is the component of the wave vector perpendicular to the z axis and $h = n_0H/n$ is a new variable related to the magnetic field and the refraction index. The asymptotic values of the E and h waves for large positive and negative z values are given by

$$\begin{aligned} E(z > 0) &= \exp(-iqz) + R_s \exp(+iqz) \\ E(z < 0) &= T_s \exp(-iq_2z), \\ h(z > 0) &= \exp(-iqz) + R_p \exp(+iqz), \\ h(z < 0) &= T_p \exp(-iq_2z), \end{aligned} \tag{5}$$

for an experiment in the geometry of Fig. 1(a). Here $q = n_0(2\pi/\lambda)\cos\phi_0$ is the component of the wave vector normal to the interface. For the particular case in which $n_1 = n_0$ the reflection and transmission coefficients for the two fields E and h are given by the Fresnel formulas

$$\begin{aligned} r_{02s} &= \frac{n_0\cos\phi_0 - n_2\cos\phi_2}{n_0\cos\phi_0 + n_2\cos\phi_2}, \\ r_{02p} &= \frac{n_2\cos\phi_0 - n_0\cos\phi_2}{n_2\cos\phi_0 + n_0\cos\phi_2}, \\ t_{02s} &= 1 + r_{02s}, \\ t_{02p} &= (1 + r_{02p})\frac{n_2}{n_0}, \end{aligned} \tag{6}$$

where ϕ_0 and ϕ_2 are the angles associated with the incident and transmitted light beams, respectively (see Fig. 1). Because the Fresnel profile has the same asymptotic values of the refractive index as the profile described by Eqs. (3), the reflection coefficients R_s and R_p are simply related[3] to r_{02s} and r_{02p} by

$$\begin{aligned} R_s &= r_{02s} - \frac{1}{i2q}\int_0^\infty dz\left(\frac{2\pi}{\lambda}\right)^2(n^2 - n_0^2)E\bar{E}, \\ R_p &= r_{02p} - \frac{1}{i2q}\int_0^\infty dz\left[\left(\frac{2\pi}{\lambda}\right)^2(n^2 - n_0^2) + n\frac{d^2}{dz^2}n^{-1}\right]h\bar{h}, \end{aligned} \tag{7}$$

$\bar{E}$ and $\bar{h}$ being the field values of the Fresnel profile, i.e., when $n_1 = n_0$. At the level of the Born approximation, one linearizes Eqs. (7) by setting $\delta n = n - n_0$ and expanding to the first order in δn. This gives, after some algebra, the following result for the ellipsometric coefficient ρ:

$$\begin{aligned} \rho = \frac{r_{02p}}{r_{02s}}\Bigg[1 &+ (A - B)\int_0^\infty dz\,\delta n(z)\sin 2qz \\ &+ i(A + B)\int_0^\infty dz\,\delta n(z)\cos 2qz\Bigg], \end{aligned} \tag{8}$$

where A and B are given by

$$\begin{aligned} A &= \frac{2\pi}{\lambda}\frac{1}{\cos\phi_0}(r_{02p}^{-1} - r_{02s}^{-1}) - \frac{4\pi}{\lambda}\cos\phi_0 r_{02p}^{-1}, \\ B &= \frac{2\pi}{\lambda}\frac{1}{\cos\phi_0}(r_{02p} - r_{02s}) - \frac{4\pi}{\lambda}\cos\phi_0 r_{02p}. \end{aligned} \tag{9}$$

The real and imaginary parts of the ellipsometry coefficients are thus related to the sine and cosine Fourier transforms of the refractive-index profile. This profile can be extracted from the ellipsometry data in the cases in which an inverse Fourier transform can be accurately performed. This condition is generally fulfilled when the profile extends over a distance many times larger than the wavelength of the light wave. In the reverse case (thin profiles) one can expand the arguments of the sine and cosine Fourier transforms for small-q vectors. The successive coefficients of the expansion are then related to the Γ_i's (the i moments of the profile), defined by

$$\Gamma_i = \int_0^\infty dz z^i \delta n(z). \tag{10}$$

The second geometry that we consider in this section [see Fig. 1(b)] corresponds to the same profile as in Eqs. (3) but with the light beam traveling toward the positive values of z. The asymptotic forms of the fields E and h are in this case given by

$$\begin{aligned} E(z < 0) &= \exp(+iq_2z) + R_s \exp(-iq_2z), \\ E(z > 0) &= T_s \exp(+iqz), \\ h(z < 0) &= \exp(+iq_2z) + R_p \exp(-iq_2z), \\ h(z > 0) &= T_p \exp(+iqz), \end{aligned} \tag{11}$$

with $q_2 = n_2(2\pi/\lambda)\cos\phi_2$. As above, the transmission and reflection coefficients can be related to the bare coefficients of the Fresnel profile, r_{20s} and r_{20p} (note the inversion of the indices, indicating that the light beam is now

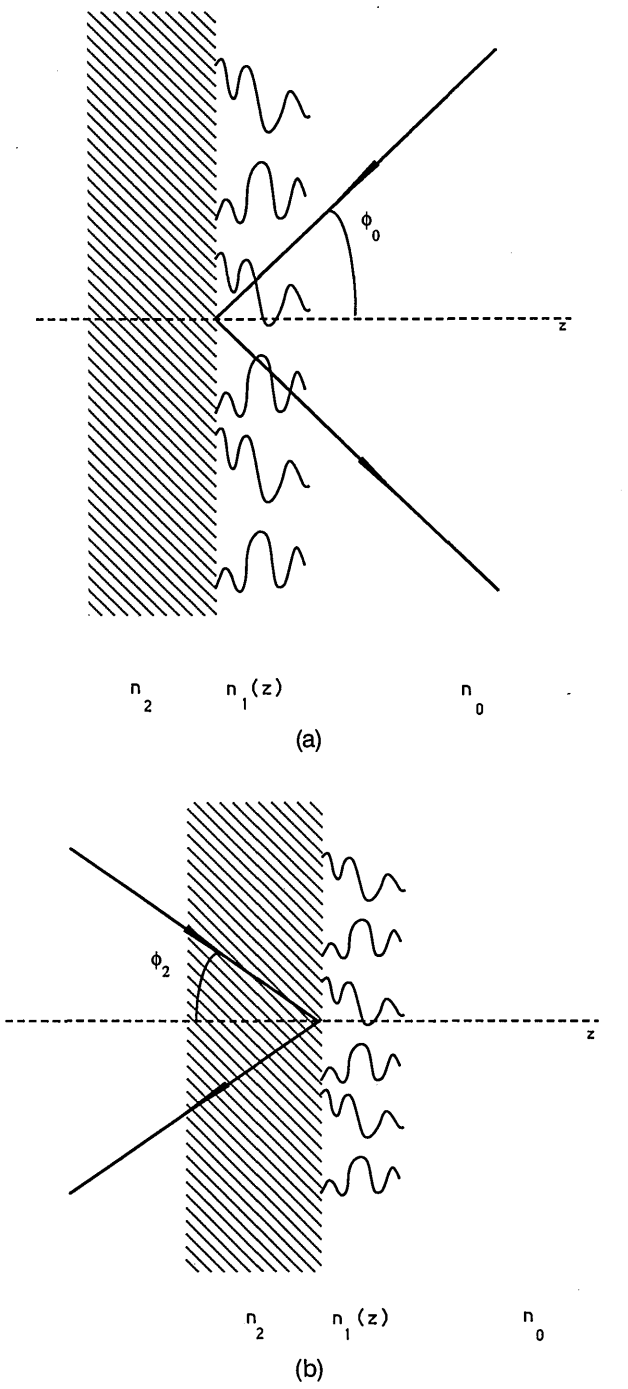

Fig. 1. (a) Experimental configuration for which the light beam travels from the liquid to the solid substrate. $n_2 > n_0$, and total reflection occurs only for grazing incidence, $\phi_0 \to \pi/2$. (b) Experimental configuration for which the light beam travels from the solid substrate to the liquid medium. $n_2 > n_0$, and total reflection occurs at a finite angle $0 < \phi_t < \pi/2$.

traveling from region 2 to region 0):

$$R_s = r_{20s} - \frac{1}{i2q_2}\int_{-\infty}^{0} dz\left(\frac{2\pi}{\lambda}\right)^2 (n^2 - n_0^2)E\bar{E},$$

$$R_p = r_{20p} - \frac{1}{i2q_2}\int_{-\infty}^{0} dz\left[\left(\frac{2\pi}{\lambda}\right)^2 (n^2 - n_0^2) + n\frac{d^2}{dz^2}n^{-1}\right]h\bar{h}. \tag{12}$$

Performing the expansion to first order in δn leads to

$$\rho = \frac{r_{20p}}{r_{20s}}\left[1 + (A - B)\int_0^\infty dz\,\delta n \sin 2qz + i(A - B)\int_0^\infty dz\,\delta n \cos 2qz\right], \tag{13}$$

where A and B are given by Eqs. (9) if one replaces ϕ_0, r_{02s}, and r_{02p} by, respectively, ϕ_2, r_{20s}, and r_{20p}. As above, the real and imaginary parts of ρ are related to the sine and cosine Fourier transforms of the refractive-index profile. The fundamental difference is that, in this geometry, the wave vector q is related to the incidence angle ϕ_2 by

$$q = \frac{2\pi}{\lambda}\left(n_0^2 - n_2^2 \sin^2 \phi_2\right)^{1/2} \tag{14}$$

and vanishes thus for a finite angle (the angle of total reflection), allowing in practice for a much more precise scanning of the small-q region.

B. Ellipsometric Effective Thickness in the Born Approximation

Here we apply the Born approximation to the ellipsometric coefficient obtained for a uniform layer. In this case the profile is given by Eqs. (2), and there is a exact solution[4] for ρ that can be written, in the first geometry [see Fig. 1(a)], as

$$\rho = \frac{r_{02p}}{r_{02s}}\left[\frac{1 + (X - 1)\dfrac{r_{12p}}{r_{01p} + r_{12p}}}{1 + (X - 1)\dfrac{r_{01p}r_{12p}}{1 + r_{01p}r_{12p}}} \times \frac{1 + (X - 1)\dfrac{r_{01s}r_{12s}}{1 + r_{01s}r_{12s}}}{1 + (X - 1)\dfrac{r_{12s}}{r_{01s} + r_{12s}}}\right], \tag{15}$$

where we have introduced $X = \cos 2qd - i \sin 2qd$ and where the reflection coefficients r_{ijs} and r_{ijp} can be obtained from Eqs. (6) by using the corresponding indices. To perform the expansion of Eq. (15) to the first order in $\delta n = n_1 - n_0$, we first remark that $\cos \phi_1 = 1/n_1(n_1^2 - n_2^2 + n_2^2 \cos^2 \phi_2)^{1/2}$ and then get

$$\rho = \frac{r_{02p}}{r_{02s}}\left\{1 + \delta n\left[\frac{A - B}{q}(1 - \cos 2qd) - i\frac{A + B}{q}\sin 2qd\right]\right\}. \tag{16}$$

By direct comparison of Eqs. (8) and (16) we can finally extract two equations relating the effective thickness $d(q)$ and refractive index $\delta n(q)$ to the Fourier transforms of the profile:

$$\delta n(q)[1 - \cos 2qd(q)] = 2q\int_0^\infty dz\,\delta n \sin 2qz,$$

$$\delta n(q)\sin 2qd(q) = 2q\int_0^\infty dz\,\delta n \cos 2qz. \tag{17}$$

A similar procedure allows for the derivation of the corresponding result for the second geometry:

$$\rho = \frac{r_{20p}}{r_{20s}}\left\{1 + \delta n\left[\frac{A - B}{q}(1 - \cos 2qd) - i\frac{A - B}{q}\sin 2qd\right]\right\}. \tag{18}$$

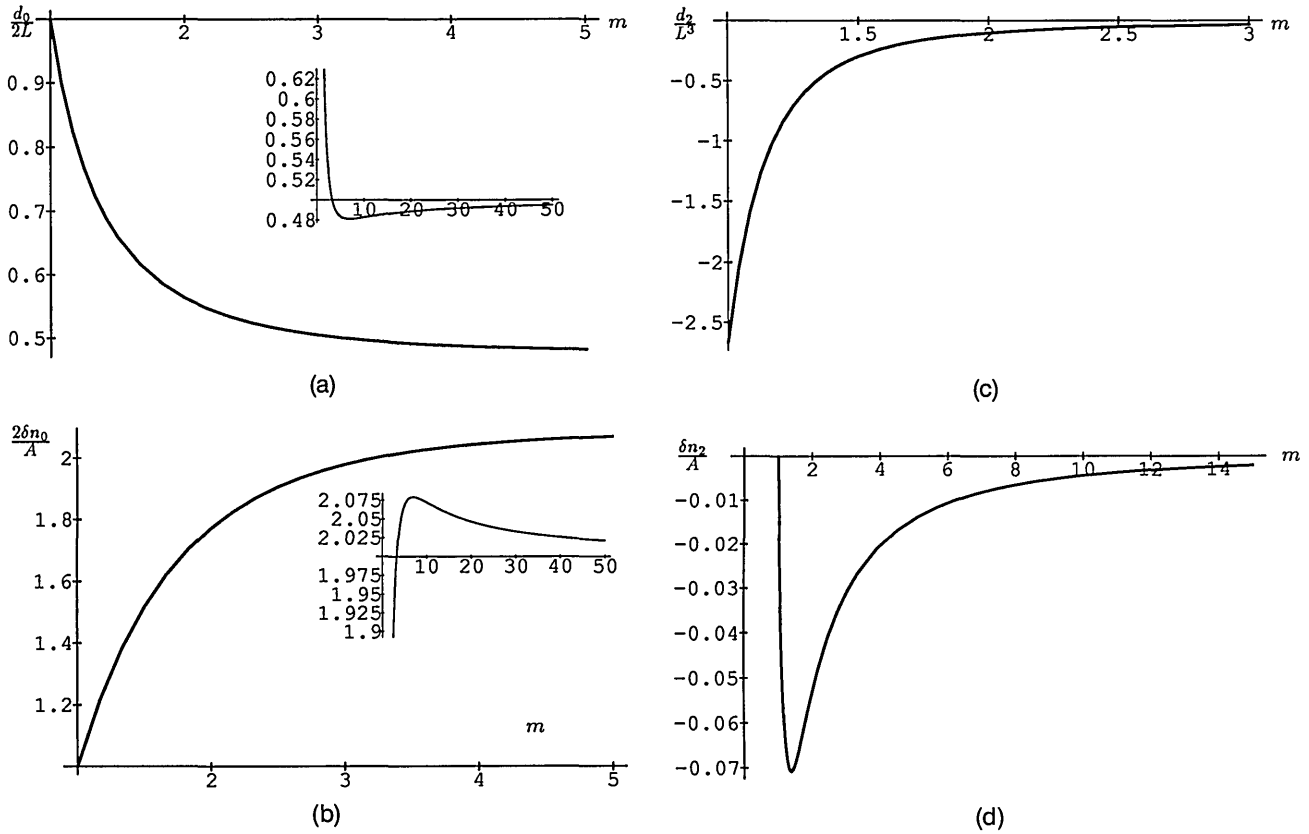

Fig. 2. Values of the four coefficients in the small-q expansion for the family of profiles $\delta n \sim A_m \exp[-(z/L_0)^m]$ introduced in the text: (a) $d_0/(2L)$, (b) $2\delta n_0/A$, (c) d_2/L^3, (d) $\delta n_2/A$.

which, by comparison with Eq. (13), leads again to Eqs. (17). These relations are our central result, relating the (q-dependent) effective ellipsometric thickness $d(q)$ and refractive index $\delta n(q)$ to the Fourier transforms of the refractive-index profile. The important point here is that Eqs. (17) hold in both geometries, leading to a preferential choice of the second geometry (where total reflexion occurs and q vanishes at a finite angle) when ellipsometry measurements of thin layers (with a profile extending over a distance smaller than the wavelength of light) are to be performed. For these layers (see Section 3 below) it is interesting to perform a small-q expansion of the effective thicknesses and indices. This small-q expansion can be obtained in both geometries, but in the first one the experiments need to be performed at grazing incidence, which is indeed difficult. On the contrary, the limit of $q = 0$ is easily obtained in the second geometry, where q vanishes at a finite angle, which is the total reflection angle.

3. SMALL-Q EXPANSION FOR THE EFFECTIVE THICKNESS AND INDEX OF THIN FILMS

In this section we restrict our attention to the family of thin layers for which the characteristic thickness is smaller than the wavelength. In this case it is convenient to expand the effective thickness and refractive index in powers of the wave vector q by setting

$$d(q) = d_0 + qd_1 + q^2 d_2^2 + \ldots,$$
$$\delta n(q) = \delta n_0 + q\delta n_1 + q^2 \delta n_2 + \ldots. \quad (19)$$

The different coefficients d_i and δn_i can be calculated by combining the precedent equations with Eqs. (17) and (10). Only the even coefficients have nonzero values, and they read as

$$d_0 = 2\alpha_1,$$
$$d_2 = \tfrac{4}{3}(\alpha_1\alpha_2 - 2\alpha_1^3 - \alpha_3),$$
$$\delta n_0 = \frac{\Gamma_0}{d_0},$$
$$\delta n_2 = \Gamma_0\left(\frac{4}{3}\alpha_1 - \frac{\alpha_2}{\alpha_1} - \frac{d_2}{3\alpha_1^2}\right), \quad (20)$$

where we have introduced the new variable, $\alpha_i = \Gamma_i/\Gamma_0$. The coefficient d_0 was previously expressed by Charmet and de Gennes, who did not, however, perform a systematic expansion. The experimental data of $d(q)$ and $\delta n(q)$ are therefore described at low q by a parabola—higher-order expansions can be straightforwardly derived from Eqs. (17). Note that, consistently, d_2 and δn_2 vanish for the step profile. From the four coefficients associated with the two experimental parabolas one can, by inverting the set of Eqs. (20), obtain the four first moments of the refractive-index profile:

$$\Gamma_0 = \delta n_0 d_0,$$
$$\Gamma_1 = \tfrac{1}{2}\delta n_0 d_0^2,$$
$$\Gamma_2 = \tfrac{1}{3}d_0^3\delta n_0 - \tfrac{1}{2}\delta n_0 d_2 - \tfrac{1}{2}d_0\delta n_2,$$
$$\Gamma_3 = \tfrac{1}{4}d_0^4\delta n_0 - \tfrac{3}{4}d_0^2\delta n_2 - \tfrac{3}{2}d_2 d_0\delta n_0. \quad (21)$$

A useful illustration of the possibilities of analysis given by this method is provided by the family of profiles

$$\delta n(z) = A_m \exp[-(z/L_0)^m], \tag{22}$$

where $A_m = mA/\Gamma(1/m)$ is chosen such that the first moment Γ_1 is the same for all the exponents $m > 1$ [$\Gamma(n)$ is the usual gamma function]. In the limit of large exponents m, this profile approaches the step function. In this sense m acts as a control parameter that tunes the hardness of the profile front. In Fig. 2 we plot the values of the four coefficients of the parabolas associated with the effective thickness and refractive index as a function of m. These coefficients rapidly approach (in practice for m larger than 3) their asymptotic values $d_0 = L_0$, $d_2 = 0$, $\delta n_0 = A$, and $\delta n_2 = 0$. It is important to note that the largest values of the second-order coefficients d_2 and δn_2 are obtained for profiles with $m < 2$. Interestingly, the pure exponential profile ($m = 1$) also has a zero δn_2, but, generally speaking, the strongest variations of the effective thickness and index are expected for all profiles that depart substantially from a step function.

Another important class of functional forms describing the index variation of the interfacial region is found in critical phenomena[5] and polymer[6] systems, in which one often deals with profiles of the type

$$\delta n(z) = z^{-\alpha}, \qquad a \ll z \ll L, \tag{23}$$

where a and L are, respectively, the lower and upper cutoffs for the profile. One usually also has $L \gg a$. In the case of polymer adsorption in a good solvent[7] we have $\alpha = 4/3$. It follows that the coefficients d_0 and d_2 defined in Eqs. (20) are given by

$$d_0 \simeq L^{2/3} \sim N^{2/5},$$
$$d_2 \simeq -\tfrac{1}{6}L^{8/3} \sim N^{8/5}, \tag{24}$$

where we have used the relation $L \sim N^{3/5}a$, which defines the size of a polymer chain in a good solvent as a function of the chain's polymerization index N and the size of a monomer. There is already some experimental evidence[8,9] for the variation of the coefficient d_0 with the polymerization index. New investigations concerning the coefficient d_2 would bring further clarification on the issue of polymer adsorption profiles.

4. NUMERICAL INTEGRATION OF THE MAXWELL EQUATIONS FOR THE PARABOLIC PROFILE

Recently some interest in parabolic profiles has been raised by theoretical predictions concerning the concentration profile of grafted polymer layers. These layers, formed by linear polymers having one extremity grafted to a surface, were predicted at first to have a steplike index profile[10] and more recently to have a parabolic profile,[11] given by

$$\delta n(z) = \delta n[1 - (z/L)^2] \qquad 0 < z < L, \tag{25}$$

where L depends on the polymerization index of the polymers and on the surface density of grafted polymer heads. Testing the possibility of actually differentiating the two predicted profiles by ellipsometry, we carried out a numerical integration of the Maxwell equations for the parabolic profile in different geometries: the two cases of Fig. 1, reflection upon a metallic mirror and a prism coated with a thin silver film (plasmon configuration).

For the numerical calculation we used the matrix formulation for the optical properties of an inhomogeneous medium as described by Abelès,[12] which divides the profile into a series of thin sublayers where the refractive index is constant. The results, presented in Fig. 3(a), are obtained in the first geometry [Fig. 1(a)], i.e., with the light traveling from the polymer solution with $n_0 = 1.33$ to the glass substrate with $n_2 = 1.55$. The grafted polymer layer has an index profile $n_0 + \delta n(z)$ given by Eq. (25), where $L = 498$ Å. The wavelength of light in air is 6000 Å, and the angle of incidence varies between 20° and 80°. Several values for δn have been used to test the domain of validity of the Born approximation.

A classical comparison of the plain ellipsometry coefficients Δ and ψ concludes with great difficulty in separating the two configurations, the differences being of the order of the experimental resolution of the technique. Nevertheless, any deviation from the step profile should induce an angle dependence in the effective thickness of the layer. Combining Eqs. (20) and (25), we find that

$$d_0 = \frac{3}{4}L,$$
$$d_2 = -\frac{7}{960}L^3. \tag{26}$$

Thus there is a weak variation of the effective thickness with q. In Fig. 3(a) we show the value of the effective thickness of the parabolic layer described above, calculated from the ellipsometric coefficients obtained by our

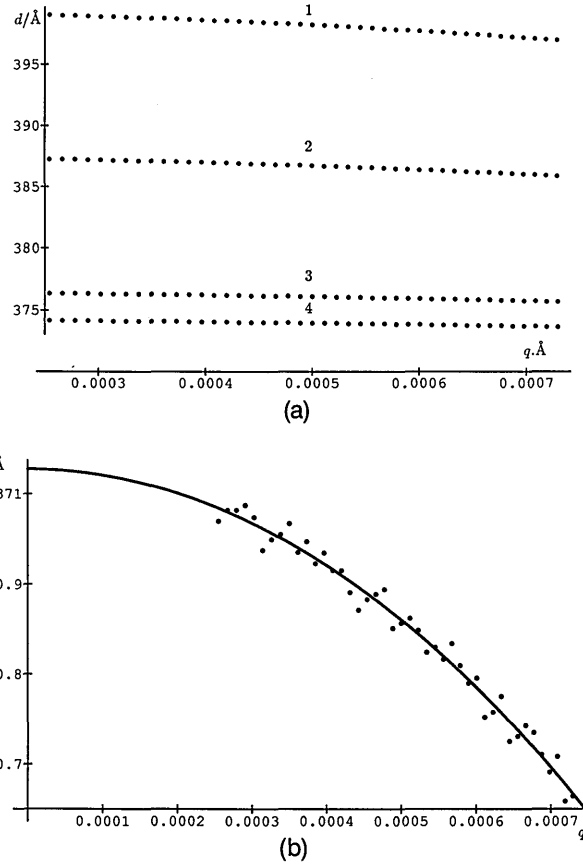

Fig. 3. (a) Variation of the effective thickness of the parabolic layer for different indices: 1, $\delta n = 0.1$; 2, $\delta n = 0.061$; 3, $\delta n = 0.2$; 4, $\delta n = 0.01$. (b) Extrapolation of the precedent set of values to zero contrast, $\delta n = 0$.

numerical integration method. To obtain the correct perturbation limit in which Eqs. (20) hold, first we calculated $d(q)$ for several values of δn and then extrapolated to $\delta n = 0$ [Fig. 3(b)]. The fit of these experimental points by a parabola gives

$$d_0 = 0.747L,$$
$$d_2 = -0.0053L^3, \tag{27}$$

values that are in reasonably good agreement with the predicted ones, especially considering that the perturbation parameter qL is not very small ($0.15 < qL < 0.35$). Better agreement should be obtained for a simulation in which total reflection is possible.

5. CONCLUSIONS

We have analyzed the angle dependence of the effective refractive index and layer thickness of an inhomogeneous layer calculated from the usual ellipsometric parameters ψ and Δ. The effective refractive index and layer thickness describe an equivalent homogeneous layer that, for a given wavelength and incident angle, would have the same reflectance as the inhomogeneous layer. At the level of the linear Born approximation the angle dependence of the effective refractive index and layer thickness is simply related to the Fourier transforms of the index profile. The linear approximation holds only asymptotically, i.e., in the limit of zero optical contrast. For this reason the actual layer parameters can be obtained by a contrast-variation method, followed by an extrapolation to zero contrast. For layers that extend from the surface over a distance much smaller than the wavelength of light a convenient analysis of the results can be obtained by a small-q expansion, where q is the component of the incident vector normal to the surface. In most experiments it is not possible to explore the layer structure from incidence angles larger than 80°–85°. To work at small-q values it is thus much better to perform experiments in configurations in which total reflection occurs, i.e., where q vanishes for a finite angle. From the functional variation of the effective parameters with the incident vector q it is possible to extract successive moments of the index profile. For instance, at the lower level in the q expansion the functional forms are parabolas, and the four first moments can be obtained.

The influence of the profile steepness on the q dependence of the effective parameters can be discussed by studying the family of profiles $\delta n \sim A_m \exp[-(z/L_0)^m]$ for which the front thickness is of order of L_0/m. Generally speaking, the only noticeable departures from the step-profile characteristics occur for m close to unity, i.e., when the profile front varies over the entire profile thickness.

We have also discussed the mass dependence of the effective thickness of an adsorbed polymer layer. It turns out that the second coefficient in the q expansion of the effective thickness is much more sensitive to variations in the polymer mass than the first coefficient ($N^{8/5}$ instead of $N^{2/5}$). Further experiments or a new analysis of the available data could provide useful information about these adsorbed polymer systems.

Finally, a brief comparison of our predictions with the simulated ellipsometric data on a parabolic profile describing a grafted polymer layer brought us to the conclusion that this technique should be able to distinguish between a step profile and a parabolic one—a matter of some controversy in which grafted polymer layers are concerned.

ACKNOWLEDGMENTS

We thank F. Abelès for helpful comments. This work was funded in part by European Economic Community grant SC1 0288-C.

REFERENCES

1. R. M. A. Azzam and N. M. Bashara, *Ellipsometry and Polarized Light* (North-Holland, Amsterdam, 1977).
2. J. C. Charmet and P. G. de Gennes, J. Opt. Soc. Am. **73,** 1977 (1983).
3. J. G. Lekner, *Theory of Reflection* (Nijhoff, Dordrecht, The Netherlands, 1978), Chap. 2.
4. F. L. McCrackin and J. P. Colson, *Ellipsometry in the Measurement of Surface and Thin Films,* NBS Misc. Publ. (1964).
5. K. Binder, *Phase Transitions and Critical Phenomena* (Academic, Orlando, Fla., 1983), Vol. 10.
6. P. G. de Gennes, *Scaling Concepts in Polymer Physics* (Cornell U. Press, Ithaca, N.Y., 1978).
7. P. G. de Gennes, Macromolecules **14,** 1637 (1981).
8. K. Kawaguchi, K. Hayakawa, and A. Takahashi, Macromolecules **16,** 631 (1983).
9. K. Kawaguchi, K. Hayashi, and A. Takahashi, Macromolecules **17,** 2066 (1984).
10. S. Alexander, J. Phys. (Paris) **38,** 983 (1977).
11. S. Milner, T. Witten, and M. Cates, Europhys. Lett. **5,** 413 (1988).
12. F. Abelès, Opt. Acta **4,** 42 (1957).